

Observation of a New $X(3872)$ Production Process $e^+e^- \rightarrow \omega X(3872)$

M. Ablikim¹, M. N. Achasov^{12,b}, P. Adlarson⁷², M. Albrecht⁴, R. Aliberti³³, A. Amoroso^{71A,71C}, M. R. An³⁷, Q. An^{68,55}, Y. Bai⁵⁴, O. Bakina³⁴, R. Baldini Ferroli^{27A}, I. Balossino^{28A}, Y. Ban^{44,g}, V. Batozskaya^{1,42}, D. Becker³³, K. Begzsuren³⁰, N. Berger³³, M. Bertani^{27A}, D. Bettoni^{28A}, F. Bianchi^{71A,71C}, E. Bianco^{71A,71C}, J. Bloms⁶⁵, A. Bortone^{71A,71C}, I. Boyko³⁴, R. A. Briere⁵, A. Brueggemann⁶⁵, H. Cai⁷³, X. Cai^{1,55}, A. Calcaterra^{27A}, G. F. Cao^{1,60}, N. Cao^{1,60}, S. A. Cetin^{59A}, J. F. Chang^{1,55}, W. L. Chang^{1,60}, G. R. Che⁴¹, G. Chelkov^{34,a}, C. Chen⁴¹, Chao Chen⁵², G. Chen¹, H. S. Chen^{1,60}, M. L. Chen^{1,55,60}, S. J. Chen⁴⁰, S. M. Chen⁵⁸, T. Chen^{1,60}, X. R. Chen^{29,60}, X. T. Chen^{1,60}, Y. B. Chen^{1,55}, Z. J. Chen^{24,h}, W. S. Cheng^{71C}, S. K. Choi⁵², X. Chu⁴¹, G. Cibinetto^{28A}, F. Cossio^{71C}, J. J. Cui⁴⁷, H. L. Dai^{1,55}, J. P. Dai⁷⁶, A. Dbeyssi¹⁸, R. E. de Boer⁴, D. Dedovich³⁴, Z. Y. Deng¹, A. Denig³³, I. Denysenko³⁴, M. Destefanis^{71A,71C}, F. De Mori^{71A,71C}, Y. Ding³⁸, Y. Ding³², J. Dong^{1,55}, L. Y. Dong^{1,60}, M. Y. Dong^{1,55,60}, X. Dong⁷³, S. X. Du⁷⁸, Z. H. Duan⁴⁰, P. Egorov^{34,a}, Y. L. Fan⁷³, J. Fang^{1,55}, S. S. Fang^{1,60}, W. X. Fang¹, Y. Fang¹, R. Farinelli^{28A}, L. Fava^{71B,71C}, F. Feldbauer⁴, G. Felici^{68,55}, C. Q. Feng^{68,55}, J. H. Feng⁵⁶, K. Fischer⁶⁰, M. Fritsch⁴, C. Fritzsche⁶⁵, C. D. Fu¹, H. Gao⁶⁰, Y. N. Gao^{44,g}, Yang Gao^{68,55}, S. Garbolino^{71C}, I. Garzia^{28A,28B}, P. T. Ge⁷³, Z. W. Ge⁴⁰, C. Geng⁵⁶, E. M. Gersabeck⁶⁴, A. Gilman⁶⁶, K. Goetzen¹³, L. Gong³⁸, W. X. Gong^{1,55}, W. Gradl³³, M. Greco^{71A,71C}, L. M. Gu⁴⁰, M. H. Gu^{1,55}, Y. T. Gu¹⁵, C. Y. Guan^{1,60}, A. Q. Guo^{29,60}, L. B. Guo³⁹, R. P. Guo⁴⁶, Y. P. Guo^{11,f}, A. Guskov^{34,a}, W. Y. Han³⁷, X. Q. Hao¹⁹, F. A. Harris⁶², K. K. He⁵², K. L. He^{1,60}, F. H. Heinsius⁴, C. H. Heinz³³, Y. K. Heng^{1,55,60}, C. Herold⁵⁷, G. Y. Hou^{1,60}, Y. R. Hou⁶⁰, Z. L. Hou¹, H. M. Hu^{1,60}, J. F. Hu^{53,i}, T. Hu^{1,55,60}, Y. Hu¹, G. S. Huang^{68,55}, K. X. Huang⁵⁶, L. Q. Huang^{29,60}, X. T. Huang⁴⁷, Y. P. Huang¹, Z. Huang^{44,g}, T. Hussain⁷⁰, N. Hüsken^{26,33}, W. Imoehl²⁶, M. Irshad^{68,55}, J. Jackson²⁶, S. Jaeger⁴, S. Janchiv³⁰, E. Jang⁵², J. H. Jeong⁵², Q. Ji¹, Q. P. Ji¹⁹, X. B. Ji^{1,60}, X. L. Ji^{1,55}, Y. Y. Ji⁴⁷, Z. K. Jia^{68,55}, P. C. Jiang^{44,g}, S. S. Jiang³⁷, X. S. Jiang^{1,55,60}, Y. Jiang⁶⁰, J. B. Jiao⁴⁷, Z. Jiao²², S. Jin⁴⁰, Y. Y. Jin⁶¹, M. Q. Jing^{1,60}, T. Johansson⁷², S. Kabana³¹, N. Kalantar-Nayestanaki⁶¹, X. L. Kang⁹, X. S. Kang³⁸, R. Kappert⁶¹, M. Kavatsyuk⁶¹, B. C. Ke⁷⁸, I. K. Keshk⁴, A. Khokuz⁶⁵, R. Kiuchi¹, R. Kliemt¹³, L. Koch³⁵, O. B. Kolcu^{59A}, B. Kopf⁴, M. Kuemmel⁴, M. Kuessner⁴, A. Kupsc^{42,72}, W. Kühn³⁵, J. J. Lane⁶⁴, J. S. Lange³⁵, P. Larin¹⁸, A. Lavanian²⁵, L. Lavezzi^{71A,71C}, T. T. Lei^{68,k}, Z. H. Lei^{68,55}, H. Leithoff³³, M. Lellmann³³, T. Lenz³³, C. Li⁴¹, C. Li⁴⁵, C. H. Li³⁷, Cheng Li^{68,55}, D. M. Li⁷⁸, F. Li^{1,55}, G. Li¹, H. Li⁴⁹, H. Li^{68,55}, H. B. Li^{1,60}, H. J. Li¹⁹, H. N. Li^{53,i}, J. Q. Li⁴, J. S. Li⁵⁶, J. W. Li⁴⁷, Ke Li¹, L. J. Li^{1,60}, L. K. Li¹, Lei Li³, M. H. Li⁴¹, P. R. Li^{36,j,k}, S. X. Li¹¹, S. Y. Li⁵⁸, T. Li⁴⁷, W. D. Li^{1,60}, W. G. Li¹, X. H. Li^{68,55}, X. L. Li⁴⁷, Xiaoyu Li^{1,60}, Y. G. Li^{44,g}, Z. X. Li¹⁵, Z. Y. Li⁵⁶, C. Liang⁴⁰, H. Liang^{1,60}, H. Liang³², H. Liang^{68,55}, Y. F. Liang⁵¹, Y. T. Liang^{29,60}, G. R. Liao¹⁴, L. Z. Liao⁴⁷, J. Libby²⁵, A. Limphirat⁵⁷, C. X. Lin⁵⁶, D. X. Lin^{29,60}, T. Lin¹, B. J. Liu¹, C. Liu³², C. X. Liu¹, D. Liu^{18,68}, F. H. Liu⁵⁰, Fang Liu¹, Feng Liu⁶, G. M. Liu^{53,i}, H. Liu^{36,j,k}, H. B. Liu¹⁵, H. M. Liu^{1,60}, Huanhuan Liu¹, Huihui Liu²⁰, J. B. Liu^{68,55}, J. L. Liu⁶⁹, J. Y. Liu^{1,60}, K. Liu¹, K. Y. Liu³⁸, Ke Liu²¹, L. Liu^{68,55}, Lu Liu⁴¹, M. H. Liu^{11,f}, P. L. Liu¹, Q. Liu⁶⁰, S. B. Liu^{68,55}, T. Liu^{11,f}, W. K. Liu⁴¹, W. M. Liu^{68,55}, X. Liu^{36,j,k}, Y. Liu^{36,j,k}, Y. B. Liu⁴¹, Z. A. Liu^{1,55,60}, Z. Q. Liu⁴⁷, X. C. Lou^{1,55,60}, F. X. Lu⁵⁶, H. J. Lu²², J. G. Lu^{1,55}, X. L. Lu¹, Y. Lu⁷, Y. P. Lu^{1,55}, Z. H. Lu^{1,60}, C. L. Luo³⁹, M. X. Luo⁷⁷, T. Luo^{11,f}, X. L. Luo^{1,55}, X. R. Lyu⁶⁰, Y. F. Lyu⁴¹, F. C. Ma³⁸, H. L. Ma¹, L. L. Ma⁴⁷, M. M. Ma^{1,60}, Q. M. Ma¹, R. Q. Ma^{1,60}, R. T. Ma⁶⁰, X. Y. Ma^{1,55}, Y. Ma^{44,g}, F. E. Maas¹⁸, M. Maggiora^{71A,71C}, S. Maldaner⁴, S. Malde⁶⁶, Q. A. Malik⁷⁰, A. Mangoni^{27B}, Y. J. Mao^{44,g}, Z. P. Mao¹, S. Marcello^{71A,71C}, Z. X. Meng⁶³, J. G. Messchendorp^{13,61}, G. Mezzadri^{28A}, H. Miao^{1,60}, T. J. Min⁴⁰, R. E. Mitchell²⁶, X. H. Mo^{1,55,60}, N. Yu. Muchnoi^{12,b}, Y. Nefedov³⁴, F. Nerling^{18,d}, I. B. Nikolaev^{12,b}, Z. Ning^{1,55}, S. Nisar^{10,l}, Y. Niu⁴⁷, S. L. Olsen⁶⁰, Q. Ouyang^{1,55,60}, S. Pacetti^{27B,27C}, X. Pan^{11,f}, Y. Pan⁵⁴, A. Pathak³², Y. P. Pei^{68,55}, M. Pelizaeus⁴, H. P. Peng^{68,55}, K. Peters^{13,d}, J. L. Ping³⁹, R. G. Ping^{1,60}, S. Plura³³, S. Pogodin³⁴, V. Prasad^{68,55}, F. Z. Qi¹, H. Qi^{68,55}, H. R. Qi⁵⁸, M. Qi⁴⁰, T. Y. Qi^{11,f}, S. Qian^{1,55}, W. B. Qian⁶⁰, Z. Qian⁵⁶, C. F. Qiao⁶⁰, J. J. Qin⁶⁹, L. Q. Qin¹⁴, X. P. Qin^{11,f}, X. S. Qin⁴⁷, Z. H. Qin^{1,55}, J. F. Qiu¹, S. Q. Qu⁵⁸, K. H. Rashid⁷⁰, C. F. Redmer³³, K. J. Ren³⁷, A. Rivetti^{71C}, V. Rodin⁶¹, M. Rolo^{71C}, G. Rong^{1,60}, Ch. Rosner¹⁸, S. N. Ruan⁴¹, A. Sarantsev^{34,c}, Y. Schelhaas³³, C. Schmier⁴, K. Schoenning⁷², M. Scodeggio^{28A,28B}, K. Y. Shan^{11,f}, W. Shan²³, X. Y. Shan^{1,60}, J. F. Shangguan⁵², L. G. Shao^{1,60}, M. Shao^{68,55}, C. P. Shen^{11,f}, H. F. Shen^{1,60}, W. H. Shen⁶⁰, X. Y. Shen^{1,60}, B. A. Shi⁶⁰, H. C. Shi^{68,55}, J. Y. Shi¹, Q. Q. Shi⁵², R. S. Shi^{1,60}, X. Shi^{1,55}, J. J. Song¹⁹, W. M. Song^{32,1}, Y. X. Song^{44,g}, S. Sosio^{71A,71C}, S. Spataro^{71A,71C}, F. Stieler³³, P. P. Su⁵², Y. J. Su⁶⁰, G. X. Sun¹, H. Sun⁶⁰, H. K. Sun¹, J. F. Sun¹⁹, L. Sun⁷³, S. S. Sun^{1,60}, T. Sun^{1,60}, W. Y. Sun³², Y. J. Sun^{68,55}, Y. Z. Sun¹, Z. T. Sun⁴⁷, Y. H. Tan⁷³, Y. X. Tan^{68,55}, C. J. Tang⁵¹, G. Y. Tang¹, J. Tang⁵⁶, L. Y. Tao⁶⁹, Q. T. Tao^{24,h}, M. Tat⁶⁶, J. X. Teng^{68,55}, V. Thoren⁷², W. H. Tian⁴⁹, Y. Tian^{29,60}, I. Uman^{59B}, B. Wang¹, B. Wang^{68,55}, B. L. Wang⁶⁰, C. W. Wang⁴⁰, D. Y. Wang^{44,g}, F. Wang⁶⁹, H. J. Wang^{36,j,k}, H. P. Wang^{1,60}, K. Wang^{1,55}, L. L. Wang¹, M. Wang⁴⁷, M. Z. Wang^{44,g}, Meng Wang^{1,60}, S. Wang^{11,f}, S. Wang¹⁴, T. Wang^{11,f}, T. J. Wang⁴¹, W. Wang⁵⁶, W. H. Wang⁷³, W. P. Wang^{68,55}, X. Wang^{44,g}, X. F. Wang^{36,j,k}, X. L. Wang^{11,f}, Y. Wang⁵⁸, Y. D. Wang⁴³, Y. F. Wang^{1,55,60}, Y. H. Wang⁴⁵, Y. Q. Wang¹, Yaqian Wang^{17,1}, Z. Wang^{1,55}, Z. Y. Wang^{1,60}, Ziyi Wang⁶⁰, D. H. Wei¹⁴, F. Weidner⁶⁵, S. P. Wen¹, D. J. White⁶⁴, U. Wiedner⁴, G. Wilkinson⁶⁶, M. Wolke⁷², L. Wollenberg⁴, J. F. Wu^{1,60}, L. H. Wu¹, L. J. Wu^{1,60}, X. Wu^{11,f}, X. H. Wu³², Y. Wu⁶⁸, Y. J. Wu²⁹, Z. Wu^{1,55}, L. Xia^{68,55}, T. Xiang^{44,g}, D. Xiao^{36,j,k}, G. Y. Xiao⁴⁰, H. Xiao^{11,f}, S. Y. Xiao¹, Y. L. Xiao^{11,f}, Z. J. Xiao³⁹, C. Xie⁴⁰, X. H. Xie^{44,g}, Y. Xie⁴⁷, Y. G. Xie^{1,55}, Y. H. Xie⁶, Z. P. Xie^{68,55}, T. Y. Xing^{1,60}, C. F. Xu^{1,60}, C. J. Xu⁵⁶, G. F. Xu¹, H. Y. Xu⁶³, Q. J. Xu¹⁶, X. P. Xu⁵², Y. C. Xu⁷⁵, Z. P. Xu⁴⁰, F. Yan^{11,f}, L. Yan^{11,f}, W. B. Yan^{68,55}, W. C. Yan⁷⁸, H. J. Yang^{48,e}, H. L. Yang³², H. X. Yang¹, Tao Yang¹, Y. F. Yang⁴¹, Y. X. Yang^{1,60}, Yifan Yang^{1,60}, M. Ye^{1,55}, M. H. Ye⁸, J. H. Yin¹, Z. Y. You⁵⁶, B. X. Yu^{1,55,60}, C. X. Yu⁴¹, G. Yu^{1,60}, T. Yu⁶⁹, X. D. Yu^{44,g}, C. Z. Yuan^{1,60}, L. Yuan², S. C. Yuan¹, X. Q. Yuan¹, Y. Yuan^{1,60}, Z. Y. Yuan⁵⁶, C. X. Yue³⁷, A. A. Zafar⁷⁰, F. R. Zeng⁴⁷, X. Zeng⁶, Y. Zeng^{24,h}, X. Y. Zhai³², Y. H. Zhan⁵⁶, A. Q. Zhang^{1,60}, B. L. Zhang^{1,60},

B. X. Zhang¹, D. H. Zhang⁴¹, G. Y. Zhang¹⁹, H. Zhang⁶⁸, H. H. Zhang³², H. H. Zhang⁵⁶, H. Q. Zhang^{1,55,60}, H. Y. Zhang^{1,55}, J. L. Zhang⁷⁴, J. Q. Zhang³⁹, J. W. Zhang^{1,55,60}, J. X. Zhang^{36,j,k}, J. Y. Zhang¹, J. Z. Zhang^{1,60}, Jianyu Zhang^{1,60}, Jiawei Zhang^{1,60}, L. M. Zhang⁵⁸, L. Q. Zhang⁵⁶, Lei Zhang⁴⁰, P. Zhang¹, Q. Y. Zhang^{37,78}, Shuihan Zhang^{1,60}, Shulei Zhang^{24,h}, X. D. Zhang⁴³, X. M. Zhang¹, X. Y. Zhang⁴⁷, X. Y. Zhang⁵², Y. Zhang⁶⁶, Y. T. Zhang⁷⁸, Y. H. Zhang^{1,55}, Yan Zhang^{68,55}, Yao Zhang¹, Z. H. Zhang¹, Z. L. Zhang³², Z. Y. Zhang⁴¹, Z. Y. Zhang⁷³, G. Zhao¹, J. Zhao³⁷, J. Y. Zhao^{1,60}, J. Z. Zhao^{1,55}, Lei Zhao^{68,55}, Ling Zhao¹, M. G. Zhao⁴¹, S. J. Zhao⁷⁸, Y. B. Zhao^{1,55}, Y. X. Zhao^{29,60}, Z. G. Zhao^{68,55}, A. Zhemchugov^{34,a}, B. Zheng⁶⁹, J. P. Zheng^{1,55}, Y. H. Zheng⁶⁰, B. Zhong³⁹, C. Zhong⁶⁹, X. Zhong⁵⁶, H. Zhou⁴⁷, L. P. Zhou^{1,60}, X. Zhou⁷³, X. K. Zhou⁶⁰, X. R. Zhou^{68,55}, X. Y. Zhou³⁷, Y. Z. Zhou^{11,f}, J. Zhu⁴¹, K. Zhu¹, K. J. Zhu^{1,55,60}, L. X. Zhu⁶⁰, S. H. Zhu⁶⁷, S. Q. Zhu⁴⁰, T. J. Zhu⁷⁴, W. J. Zhu^{11,f}, Y. C. Zhu^{68,55}, Z. A. Zhu^{1,60}, J. H. Zou¹, J. Zu^{68,55}

(BESIII Collaboration)

¹ Institute of High Energy Physics, Beijing 100049, People's Republic of China

² Beihang University, Beijing 100191, People's Republic of China

³ Beijing Institute of Petrochemical Technology, Beijing 102617, People's Republic of China

⁴ Bochum Ruhr-University, D-44780 Bochum, Germany

⁵ Carnegie Mellon University, Pittsburgh, Pennsylvania 15213, USA

⁶ Central China Normal University, Wuhan 430079, People's Republic of China

⁷ Central South University, Changsha 410083, People's Republic of China

⁸ China Center of Advanced Science and Technology, Beijing 100190, People's Republic of China

⁹ China University of Geosciences, Wuhan 430074, People's Republic of China

¹⁰ COMSATS University Islamabad, Lahore Campus, Defence Road, Off Raiwind Road, 54000 Lahore, Pakistan

¹¹ Fudan University, Shanghai 200433, People's Republic of China

¹² G.I. Budker Institute of Nuclear Physics SB RAS (BINP), Novosibirsk 630090, Russia

¹³ GSI Helmholtzcentre for Heavy Ion Research GmbH, D-64291 Darmstadt, Germany

¹⁴ Guangxi Normal University, Guilin 541004, People's Republic of China

¹⁵ Guangxi University, Nanning 530004, People's Republic of China

¹⁶ Hangzhou Normal University, Hangzhou 310036, People's Republic of China

¹⁷ Hebei University, Baoding 071002, People's Republic of China

¹⁸ Helmholtz Institute Mainz, Staudinger Weg 18, D-55099 Mainz, Germany

¹⁹ Henan Normal University, Xinxiang 453007, People's Republic of China

²⁰ Henan University of Science and Technology, Luoyang 471003, People's Republic of China

²¹ Henan University of Technology, Zhengzhou 450001, People's Republic of China

²² Huangshan College, Huangshan 245000, People's Republic of China

²³ Hunan Normal University, Changsha 410081, People's Republic of China

²⁴ Hunan University, Changsha 410082, People's Republic of China

²⁵ Indian Institute of Technology Madras, Chennai 600036, India

²⁶ Indiana University, Bloomington, Indiana 47405, USA

²⁷ INFN Laboratori Nazionali di Frascati, (A)INFN Laboratori Nazionali di Frascati, I-00044, Frascati, Italy; (B)INFN

Sezione di Perugia, I-06100, Perugia, Italy; (C)University of Perugia, I-06100, Perugia, Italy

²⁸ INFN Sezione di Ferrara, (A)INFN Sezione di Ferrara, I-44122, Ferrara, Italy; (B)University of Ferrara, I-44122, Ferrara, Italy

²⁹ Institute of Modern Physics, Lanzhou 730000, People's Republic of China

³⁰ Institute of Physics and Technology, Peace Avenue 54B, Ulaanbaatar 13330, Mongolia

³¹ Instituto de Alta Investigacion, Universidad de Tarapaca, Casilla 7D, Arica, Chile

³² Jilin University, Changchun 130012, People's Republic of China

³³ Johannes Gutenberg University of Mainz, Johann-Joachim-Becher-Weg 45, D-55099 Mainz, Germany

³⁴ Joint Institute for Nuclear Research, 141980 Dubna, Moscow region, Russia

³⁵ Justus-Liebig-Universitaet Giessen, II. Physikalisches Institut, Heinrich-Buff-Ring 16, D-35392 Giessen, Germany

³⁶ Lanzhou University, Lanzhou 730000, People's Republic of China

³⁷ Liaoning Normal University, Dalian 116029, People's Republic of China

³⁸ Liaoning University, Shenyang 110036, People's Republic of China

³⁹ Nanjing Normal University, Nanjing 210023, People's Republic of China

⁴⁰ Nanjing University, Nanjing 210093, People's Republic of China

⁴¹ Nankai University, Tianjin 300071, People's Republic of China

⁴² National Centre for Nuclear Research, Warsaw 02-093, Poland

⁴³ North China Electric Power University, Beijing 102206, People's Republic of China

⁴⁴ Peking University, Beijing 100871, People's Republic of China

⁴⁵ Qufu Normal University, Qufu 273165, People's Republic of China

⁴⁶ Shandong Normal University, Jinan 250014, People's Republic of China

⁴⁷ Shandong University, Jinan 250100, People's Republic of China

⁴⁸ Shanghai Jiao Tong University, Shanghai 200240, People's Republic of China

⁴⁹ Shanxi Normal University, Linfen 041004, People's Republic of China

⁵⁰ Shanxi University, Taiyuan 030006, People's Republic of China

- ⁵¹ Sichuan University, Chengdu 610064, People's Republic of China
⁵² Soochow University, Suzhou 215006, People's Republic of China
⁵³ South China Normal University, Guangzhou 510006, People's Republic of China
⁵⁴ Southeast University, Nanjing 211100, People's Republic of China
⁵⁵ State Key Laboratory of Particle Detection and Electronics, Beijing 100049, Hefei 230026, People's Republic of China
⁵⁶ Sun Yat-Sen University, Guangzhou 510275, People's Republic of China
⁵⁷ Suranaree University of Technology, University Avenue 111, Nakhon Ratchasima 30000, Thailand
⁵⁸ Tsinghua University, Beijing 100084, People's Republic of China
⁵⁹ Turkish Accelerator Center Particle Factory Group, (A)Istinye University, 34010, Istanbul, Turkey; (B)Near East University, Nicosia, North Cyprus, Mersin 10, Turkey
⁶⁰ University of Chinese Academy of Sciences, Beijing 100049, People's Republic of China
⁶¹ University of Groningen, NL-9747 AA Groningen, The Netherlands
⁶² University of Hawaii, Honolulu, Hawaii 96822, USA
⁶³ University of Jinan, Jinan 250022, People's Republic of China
⁶⁴ University of Manchester, Oxford Road, Manchester, M13 9PL, United Kingdom
⁶⁵ University of Muenster, Wilhelm-Klemm-Strasse 9, 48149 Muenster, Germany
⁶⁶ University of Oxford, Keble Road, Oxford OX13RH, United Kingdom
⁶⁷ University of Science and Technology Liaoning, Anshan 114051, People's Republic of China
⁶⁸ University of Science and Technology of China, Hefei 230026, People's Republic of China
⁶⁹ University of South China, Hengyang 421001, People's Republic of China
⁷⁰ University of the Punjab, Lahore-54590, Pakistan
⁷¹ University of Turin and INFN, (A)University of Turin, I-10125, Turin, Italy; (B)University of Eastern Piedmont, I-15121, Alessandria, Italy; (C)INFN, I-10125, Turin, Italy
⁷² Uppsala University, Box 516, SE-75120 Uppsala, Sweden
⁷³ Wuhan University, Wuhan 430072, People's Republic of China
⁷⁴ Xinyang Normal University, Xinyang 464000, People's Republic of China
⁷⁵ Yantai University, Yantai 264005, People's Republic of China
⁷⁶ Yunnan University, Kunming 650500, People's Republic of China
⁷⁷ Zhejiang University, Hangzhou 310027, People's Republic of China
⁷⁸ Zhengzhou University, Zhengzhou 450001, People's Republic of China
^a Also at the Moscow Institute of Physics and Technology, Moscow 141700, Russia
^b Also at the Novosibirsk State University, Novosibirsk, 630090, Russia
^c Also at the NRC "Kurchatov Institute", PNPI, 188300, Gatchina, Russia
^d Also at Goethe University Frankfurt, 60323 Frankfurt am Main, Germany
^e Also at Key Laboratory for Particle Physics, Astrophysics and Cosmology, Ministry of Education; Shanghai Key Laboratory for Particle Physics and Cosmology; Institute of Nuclear and Particle Physics, Shanghai 200240, People's Republic of China
^f Also at Key Laboratory of Nuclear Physics and Ion-beam Application (MOE) and Institute of Modern Physics, Fudan University, Shanghai 200443, People's Republic of China
^g Also at State Key Laboratory of Nuclear Physics and Technology, Peking University, Beijing 100871, People's Republic of China
^h Also at School of Physics and Electronics, Hunan University, Changsha 410082, China
ⁱ Also at Guangdong Provincial Key Laboratory of Nuclear Science, Institute of Quantum Matter, South China Normal University, Guangzhou 510006, China
^j Also at Frontiers Science Center for Rare Isotopes, Lanzhou University, Lanzhou 730000, People's Republic of China
^k Also at Lanzhou Center for Theoretical Physics, Lanzhou University, Lanzhou 730000, People's Republic of China
^l Also at the Department of Mathematical Sciences, IBA, Karachi, Pakistan

(Dated: December 14, 2022)

Using 4.7 fb^{-1} of e^+e^- collision data at center-of-mass energies from 4.661 to 4.951 GeV collected by the BESIII detector at the BEPCII collider, we observe the $X(3872)$ production process $e^+e^- \rightarrow \omega X(3872)$ for the first time. The significance is 7.8σ , including both the statistical and systematic uncertainties. The $e^+e^- \rightarrow \omega X(3872)$ Born cross section and the corresponding upper limit at 90% confidence level at each energy point are reported. The line shape of the cross section indicates that the $\omega X(3872)$ signals may be from the decays of some non-trivial structures.

A number of experimentally observed quarkonium-like states do not fit within the conventional quarkonium spectrum and are thus popular candidates for exotic hadrons. As the first experimentally observed quarkonium-like state in this category, the $X(3872)$ was found by Belle in the decay $B^\pm \rightarrow K^\pm \pi^+ \pi^- J/\psi$ in

2003 [1]. It was subsequently confirmed by other experiments [2–4]. After two decades of studies, its resonance parameters and quantum numbers are well measured. The mass and width are determined to be $M = 3871.65 \pm 0.06 \text{ MeV}/c^2$ and $\Gamma = 1.19 \pm 0.21 \text{ MeV}$, and the spin, parity, and C -parity quantum numbers are

$J^{PC} = 1^{++}$ [5–8]. The nature of this particle, however, is still not well understood. Due to the proximity of its mass to the $D^{*0}\bar{D}^0 + c.c.$ mass threshold, it is conjectured to have a large $D^{*0}\bar{D}^0 + c.c.$ molecular component [11]. The 2^3P_1 conventional charmonium state $\chi_{c1}(2P)$ with $J^{PC} = 1^{++}$ is another possible interpretation.

In addition to exploring the $X(3872)$ via its decays, studying its production mechanisms is another way to investigate its internal structure. Besides its production in B meson decays, the $X(3872)$ was also observed in the process $e^+e^- \rightarrow \gamma X(3872)$ at BESIII [10]. According to the analysis of the line shape of the $e^+e^- \rightarrow \gamma X(3872)$ cross section, the $X(3872)$ is produced through the radiative transition $Y(4230) \rightarrow \gamma X(3872)$. Large production rates are also observed in prompt production in pp and $p\bar{p}$ collisions [4, 12–14], with rates comparable to the production rates for conventional charmonium states, which suggests the $X(3872)$ may include a conventional charmonium $\chi_{c1}(2P)$ component. Therefore, searching for new production mechanisms will provide vital information to unravel the mysterious nature of the $X(3872)$. The hadronic transitions to the spin-triplet charmonium states $\chi_{cJ}(1P)$ via $e^+e^- \rightarrow \omega\chi_{cJ}(1P)$ ($J = 0, 1, 2$) have been observed at BESIII [15–17]. If the $X(3872)$ contains a component of the excited spin-triplet charmonium state $\chi_{c1}(2P)$, the process $e^+e^- \rightarrow \omega X(3872)$ could exist. As the center-of-mass energy (\sqrt{s}) threshold to produce $\omega X(3872)$ is about 4.654 GeV, the e^+e^- annihilation data samples taken at BESIII above this production threshold offer an excellent opportunity to search for this process.

In this Letter, we report the first observation of the new $X(3872)$ production process $e^+e^- \rightarrow \omega X(3872)$. The significance is 7.5σ , which includes both the statistical and systematic uncertainties. We use 4.7 fb^{-1} of e^+e^- annihilation data at \sqrt{s} from 4.661 to 4.951 GeV collected by the BESIII detector. We reconstruct the signal process using the decays $X(3872) \rightarrow \pi^+\pi^-J/\psi$, $J/\psi \rightarrow \ell^+\ell^-$ ($\ell = e, \mu$), $\omega \rightarrow \pi^+\pi^-\pi^0$, and $\pi^0 \rightarrow \gamma\gamma$.

The BESIII detector [18] has an effective geometrical acceptance of 93% of 4π . A helium-based main drift chamber (MDC) in a 1 T magnetic field measures the momentum and the energy loss (dE/dx) of charged particles. The resolution of the momentum is about 0.5% at 1 GeV/ c , and the resolution of the dE/dx is better than 6%. An electromagnetic calorimeter (EMC) is used to measure energies and positions with an energy resolution of 2.5% in the barrel and 5.0% in the end caps for 1.0 GeV photons. A time-of-flight system with a time resolution of 80 ps (110 ps) in the barrel (end cap) is used for particle identification together with dE/dx . A muon chamber (MUC) based on resistive plate chambers with 2 cm position resolution provides information for muon identification.

Monte Carlo (MC) samples, simulated using GEANT4-based [19] software, are used to optimize the selection

criteria, determine the detection efficiency and study the potential backgrounds. The inclusive MC samples, which include open-charm hadronic processes, continuum processes, and the effects due to initial-state-radiation (ISR), are generated with KKMC [20] in conjunction with EVTGEN [21]. The signal MC samples, $e^+e^- \rightarrow \omega X(3872)$, $X(3872) \rightarrow \rho^0 J/\psi$, $\rho^0 \rightarrow \pi^+\pi^-$, $J/\psi \rightarrow \ell^+\ell^-$ ($\ell = e, \mu$), $\omega \rightarrow \pi^+\pi^-\pi^0$, and $\pi^0 \rightarrow \gamma\gamma$, are generated with the Final State Radiation (FSR) simulated by PHOTOS[22]. Each track is required to have its point of closest approach to the beamline within 1 cm in the radial direction and within 10 cm from the interaction point along the beam direction, and to lie within the polar-angle coverage of the MDC, $|\cos\theta| < 0.93$, in the laboratory frame. Photons are reconstructed from isolated showers in the EMC, which are at least 10 degrees away from any track. The EMC energy is at least 25 MeV in the barrel ($|\cos\theta| < 0.80$) and 50 MeV in the end-caps ($0.86 < |\cos\theta| < 0.92$). In order to suppress electronic noise and energy deposits unrelated to the event, the EMC time t of the photon candidate must be in coincidence with collision events in the range $0 \leq t \leq 700$ ns.

The final state of the signal process includes six charged tracks (a lepton pair and four charged pions) and two photons. In order to improve the detection efficiency, candidate events with five or six reconstructed charged tracks are both retained. Since the leptons from the J/ψ decay have higher momentum than the pions, the momentum information is used to separate the leptons from pions. Two charged particles with momenta greater than 1.0 GeV/ c and opposite charges are identified as the lepton pair from the J/ψ decay, and the remaining tracks are each assigned a pion hypothesis. Electrons and muons are discriminated by requiring their deposited energies in the EMC to be greater than 0.8 GeV and less than 0.4 GeV, respectively. In order to suppress the continuum background, at least one muon from $J/\psi \rightarrow \mu^+\mu^-$ needs to penetrate more than three layers of the MUC. As the pions are either from the $X(3872)$ or ω and the combinatorial background shows smooth distributions in the signal regions according to a study with signal MC, all possible combinations are retained.

For the candidate events with six charged particles, the net charge is required to be zero and at least one photon is required. Instead of reconstructing the two photons from a π^0 decay directly, a kinematic fit is applied to constrain the recoiling invariant mass of the four pions and the lepton pair against the initial e^+e^- collision system to the known π^0 mass [5]. The four-momentum of the non-reconstructed π^0 is calculated from the kinematic fit. The χ^2 of the one-constraint kinematic fit is required to be less than 15. The selection criteria are optimized by maximizing $S/\sqrt{S+B}$, where the number of signal events (S) is determined with the signal MC sample based on the yield observed with an unoptimized selection in data, and the background (B) is estimated with an inclusive

MC sample. After applying these requirements, a clear signal peak is seen in the distribution of the lepton pair invariant mass $M(\ell^+\ell^-)$. The J/ψ mass window is set to be $3.07 < M(\ell^+\ell^-) < 3.13$ GeV/ c^2 , and the sideband regions are defined as $2.96 < M(\ell^+\ell^-) < 3.05$ GeV/ c^2 and $3.15 < M(\ell^+\ell^-) < 3.24$ GeV/ c^2 with a width of three times the J/ψ mass window to estimate the non- J/ψ backgrounds. The main backgrounds are processes including an η or $\psi(2S)$ in the final states, *e.g.*, $e^+e^- \rightarrow (\gamma_{\text{ISR}})\pi^+\pi^-\psi(2S)$, $\psi(2S) \rightarrow \pi^+\pi^-J/\psi$ or $\eta J/\psi$. These backgrounds are reduced by requiring all charged track combinations have $M(\pi^+\pi^-\pi^0)$ and $M(\pi^+\pi^-J/\psi)$ outside the η and $\psi(2S)$ mass windows $[0.52, 0.58]$ GeV/ c^2 and $[3.680, 3.692]$ GeV/ c^2 , respectively. The efficiency varies from 18.1% to 22.0% at different energy points. To improve the resolution, $M(\pi^+\pi^-J/\psi)$ is defined as $M(\pi^+\pi^-\ell^+\ell^-) - M(\ell^+\ell^-) + m(J/\psi)$, where $m(J/\psi)$ is the known J/ψ mass [5].

For signal candidates with one undetected charged pion, only five charged tracks are reconstructed. In this case, the net charge must be ± 1 , and at least two photons must be found. A two-constraint kinematic fit is applied to these events. The invariant mass of the two photons $M(\gamma\gamma)$ is constrained to the known π^0 mass [5], and the recoiling mass of the five tracks and the π^0 against the e^+e^- initial collision momentum is constrained to the known π^+ mass [5]. If there are more than two photons in an event, the combination with the minimum χ^2 from the kinematic fit is chosen. The χ^2 is required to be less than 25. The main backgrounds after placing these requirements are similar to the six-track case, and are suppressed using the same criteria. The inclusive MC sample, which is five times larger than the data sample, is used to study the backgrounds for the five- and six-track cases [23]. The remaining backgrounds are mainly from continuum processes, and no peaking background is observed. The efficiency varies from 5.7% to 7.1% at different energy points for the five-track case.

After applying all the selection requirements, Fig. 1 shows the distribution of $M(\pi^+\pi^-\pi^0)$ versus $M(\ell^+\ell^-)$ and $M(\pi^+\pi^-\pi^0)$ versus $M(\pi^+\pi^-J/\psi)$ with the combinations of the five- and six-track candidates from the data samples taken at $\sqrt{s} = 4.661 - 4.951$ GeV. The presence of the $e^+e^- \rightarrow \omega X(3872)$ signals can be seen around the intersection of the ω and $X(3872)$ signal regions. The ω candidates are required to have $M(\pi^+\pi^-\pi^0)$ within the ω mass window $[0.75, 0.81]$ GeV/ c^2 , and the ω sideband regions are defined as $[0.63, 0.72]$ GeV/ c^2 and $[0.84, 0.93]$ GeV/ c^2 , which are three times the signal region size. The sidebands are used to estimate the non- ω backgrounds. Figure 2 shows the $M(\pi^+\pi^-J/\psi)$ distribution after imposing the ω signal selection. A clear peak is seen around the $X(3872)$ signal region. The two-dimensional ω and J/ψ sidebands are used to check the backgrounds in the $X(3872)$ region as shown in Fig. 2, which illustrates a flat distribution.

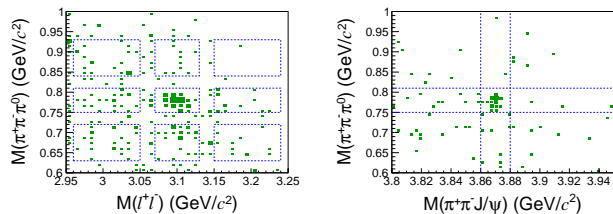


FIG. 1. Distributions of $M(\pi^+\pi^-\pi^0)$ versus $M(\ell^+\ell^-)$ (left) and $M(\pi^+\pi^-\pi^0)$ versus $M(\pi^+\pi^-J/\psi)$ (right) from the data samples at $\sqrt{s} = 4.661 - 4.951$ GeV. The central dashed box in the left plot indicates the ω and J/ψ signal regions, and the other boxes show the two-dimensional ω and J/ψ sideband regions. The dashed lines in the right plot denote the ω and $X(3872)$ signal regions after imposing the J/ψ selection.

To determine the $X(3872)$ signal yield and mass, an unbinned maximum likelihood fit is performed. The signal shape is determined by the signal MC sample with an input mass (m_{input}) of 3871.7 MeV/ c^2 [5]. The process $e^+e^- \rightarrow \gamma_{\text{ISR}}\pi^+\pi^-\psi(2S)$, $\psi(2S) \rightarrow \pi^+\pi^-J/\psi$ is used to calibrate the discrepancies in mass (Δm) and resolution ($\Delta\sigma$) between data and the MC simulation which are found to be -0.5 ± 0.2 MeV/ c^2 and 0.8 ± 0.3 MeV, respectively. The signal MC shape is convolved with a Gaussian function $G(m_g, \sigma_g)$ where m_g is free and σ_g is fixed to $\Delta\sigma$ in the fit. The background is described with a linear function with free parameters. The fit result is shown in Fig. 2. The signal yield is 24.6 ± 5.3 , and $m_g = -2.0 \pm 0.7$ MeV/ c^2 . Then, the $X(3872)$ mass is measured to be $m_x = m_{\text{input}} + m_g - \Delta m = 3870.2 \pm 0.7$ MeV/ c^2 , where the error is statistical only. Two additional background models are checked in the fit. One is to firstly fit the lower mass region $[3.8, 3.85]$ GeV/ c^2 with a linear function and the upper mass region $[3.89, 3.95]$ GeV/ c^2 with a flat distribution, respectively, and then extract the distribution of the background in the signal region with a linear interpolation between the two fitting functions, and another is a 3rd-order polynomial function. A point-to-point dissimilarity method is applied to test the goodness-of-fit [24]. The yielded p -values corresponding to the three background models are 0.93, 0.94, and 0.82, respectively, which indicate good agreement between the data and the fit results.

The significance is estimated by comparing the difference of log-likelihood values $\Delta(-2 \ln \mathcal{L})$ with and without the $X(3872)$ signal in the fit, and taking the change in the number of degrees of freedom Δndf into account. Various fit schemes *e.g.* different fitting ranges and background models are applied to extract the significance. We take the obtained smallest value 7.8σ as the significance in consideration of the systematic uncertainties. The systematic uncertainty of the mass measurement is mainly caused by the Δm error (0.2 MeV/ c^2). The uncertainty due to the mass shift in simulation is assigned to be 0.1 MeV/ c^2 according to study the signal MC sample. The

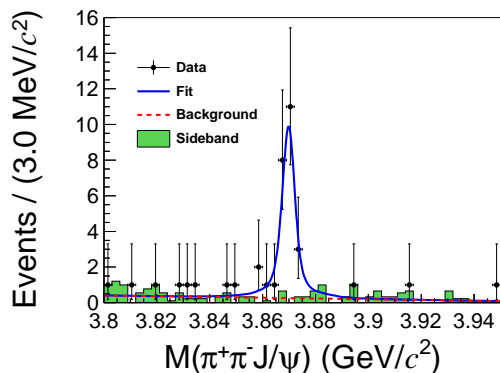


FIG. 2. Fit to the $M(\pi^+\pi^-J/\psi)$ distribution. The points with error bars are data, the solid curve is the fit result, the dashed line is the background component, and the filled histogram represents events from the ω and J/ψ two-dimensional sidebands.

uncertainties from the fit are estimated by changing different fit schemes, and obtained to be $0.1 \text{ MeV}/c^2$ in total. The total uncertainty of the $X(3872)$ mass measurement is $0.3 \text{ MeV}/c^2$ by summing all these uncertainties assuming they are independent.

The $e^+e^- \rightarrow \omega X(3872)$ Born cross section is calculated by

$$\sigma^B = \frac{N_{\text{sig}}}{\mathcal{L}_{\text{int}} \mathcal{B}_1 (\epsilon_{ee} \mathcal{B}_{ee} + \epsilon_{\mu\mu} \mathcal{B}_{\mu\mu}) (1 + \delta) \frac{1}{|1 - \Pi|^2}}, \quad (1)$$

where N_{sig} is the number of signal events; \mathcal{L}_{int} is the integrated luminosity; ϵ_{ee} and $\epsilon_{\mu\mu}$ are the detection efficiencies of the electron and muon modes, respectively; \mathcal{B}_{ee} and $\mathcal{B}_{\mu\mu}$ are the branching fractions of $J/\psi \rightarrow e^+e^-$ and $J/\psi \rightarrow \mu^+\mu^-$, respectively; \mathcal{B}_1 is the product of the branching fractions of $\omega \rightarrow \pi^+\pi^-\pi^0$ and $X(3872) \rightarrow \pi^+\pi^-J/\psi$; $(1 + \delta)$ is the ISR correction factor obtained by using a QED calculation [25] iteratively by taking the measured cross section in this analysis as an input; and $\frac{1}{|1 - \Pi|^2} = 1.055$ is the vacuum polarization factor taken from QED with an accuracy of 0.05% [26]. All branching fractions are taken from Ref. [5].

Due to the limited statistics, the signal yield (N_{sig}) at each energy point is determined by counting the number of events in the $X(3872)$ signal region $[3.86, 3.88] \text{ GeV}/c^2$. The background has been subtracted, which is estimated by using the $X(3872)$ sidebands $[3.81, 3.84] \text{ GeV}/c^2$ and $[3.91, 3.94] \text{ GeV}/c^2$. Only the $[3.81, 3.84] \text{ GeV}/c^2$ sideband region is used at $\sqrt{s} = 4.661 \text{ GeV}$ since $M(\pi^+\pi^-J/\psi)$ has a maximum allowed value of $3.914 \text{ GeV}/c^2$ at that energy. The measured N_{sig} and σ^B at each energy point are listed in Table I. The statistical significance and the upper limits of σ^B (σ_{up}^B) at the 90% confidence level at various energy points are calculated using a frequentist method with an unbounded profile likelihood treatment by assuming the numbers of

observed events in the $X(3872)$ signal and sideband regions follow a Poisson distribution [27].

The systematic uncertainties of the Born cross section measurement mainly originate from the detection efficiency, the ISR correction factor, the method of signal extraction, the integrated luminosity, and the branching fraction of $X(3872) \rightarrow \pi^+\pi^-J/\psi$. The sources of the uncertainty from the detection efficiency include the tracking, the photon reconstruction, the kinematic fit, the J/ψ mass window, the muon selection, and the signal generation model. The systematic uncertainty due to tracking is estimated with the process $e^+e^- \rightarrow \pi^+\pi^-J/\psi$ to be 1.0% per track [28]. The uncertainty of the photon reconstruction efficiency is assigned to be 1.0% per photon from the study of the process $J/\psi \rightarrow \rho^0\pi^0$ [29]. The uncertainties caused by the kinematic fit, the J/ψ mass selection, and the muon selection with the MUC are studied with the control sample of $e^+e^- \rightarrow \gamma_{\text{ISR}}\pi^+\pi^-\psi(2S)$, $\psi(2S) \rightarrow \pi^+\pi^-J/\psi$. The corresponding uncertainties are 2.8% , 4.2% , and 1.3% , respectively. The efficiencies are calculated with the signal MC samples generated with a phase space model which is flat in the distributions of ω and ρ^0 helicity angles. The uncertainty caused by the generation model and the $\eta/\psi(2S)$ veto is estimated by varying the distributions of the ω and ρ^0 helicity angles θ to be $1 \pm \cos^2\theta$. The uncertainties are found to be $(0.1-1.7)\%$. The signal yield at each energy point is obtained with the counting method; a 1.6% uncertainty is assigned comparing to that obtained with an alternative fit method at $\sqrt{s} = 4.684 \text{ GeV}$. The uncertainty due to the ISR correction factor is estimated by scaling the initial input observed line-shape within one statistical uncertainty, and the relative difference of the efficiency compared to the nominal scheme is taken as the uncertainty, which varies from 1.4% to 12.0% at different energy points. The integrated luminosity is measured with the Bhabha scattering process with an uncertainty of 1.0% [30]. The total systematic uncertainty at each energy point is obtained by adding all these systematic uncertainties in quadrature. The systematic uncertainties discussed above are summarized in Table II. The uncertainty caused by the branching fraction of $X(3872) \rightarrow \pi^+\pi^-J/\psi$ is 31.6% [5], which is listed as a separate uncertainty in the Born cross section.

In summary, based on data samples at $\sqrt{s} = 4.661 - 4.951 \text{ GeV}$ with a total integrated luminosity of 4.7 fb^{-1} collected by the BESIII detector, a new $X(3872)$ production process $e^+e^- \rightarrow \omega X(3872)$ is observed for the first time. The significance is 7.8σ , including the statistical and systematic uncertainties. The measured $X(3872)$ mass is $3870.2 \pm 0.7 \pm 0.3 \text{ MeV}/c^2$. The $e^+e^- \rightarrow \omega X(3872)$ Born cross section and the corresponding upper limit at the 90% confidence level at each energy point are reported. The line shape of the cross section indicates that the observed $\omega X(3872)$ signals may be from decays of some non-trivial structures. The production mecha-

TABLE I. Summary of the integrated luminosities (\mathcal{L}_{int}), the signal yields (N_{sig}), the product of average efficiency ($\epsilon = (\epsilon_{ee} + \epsilon_{\mu\mu})/2$) and the ISR correction factor ($1 + \delta$), the obtained $e^+e^- \rightarrow \omega X(3872)$ Born cross section or its upper limit ($\sigma_{\text{up}}^{\text{B}}$), and statistical significances at various energy points. The first uncertainties of the Born cross sections are statistical, the second are systematic, and the third are the uncertainties caused by the branching fraction of $X(3872) \rightarrow \pi^+\pi^- J/\psi$.

\sqrt{s} (GeV)	$\mathcal{L}_{\text{int}}(\text{pb}^{-1})$	N_{sig}	$\epsilon(1 + \delta)$ (%)	$\sigma^{\text{B}}(\text{pb})$	$\sigma_{\text{up}}^{\text{B}}(\text{pb})$	Significance
4.661	529.63	$0.33^{+1.36}_{-0.33}$	28.3	$0.5^{+2.1}_{-0.5} \pm 0.1 \pm 0.2$	5.6	-
4.682	1669.31	$8.00^{+3.34}_{-2.68}$	24.6	$4.6^{+1.9}_{-1.5} \pm 0.4 \pm 1.5$	11.5	3.4σ
4.699	536.45	$0.00^{+0.95}_{-0.00}$	27.0	$0.0^{+1.6}_{-0.0} \pm 0.0 \pm 0.0$	3.3	-
4.740	164.27	$1.67^{+1.77}_{-1.10}$	21.8	$10.9^{+11.6}_{-7.2} \pm 1.0 \pm 3.5$	40.6	1.0σ
4.750	367.21	$5.00^{+2.58}_{-1.92}$	22.4	$14.2^{+7.4}_{-5.5} \pm 1.4 \pm 4.5$	38.2	3.1σ
4.781	512.78	$1.00^{+1.36}_{-0.70}$	31.6	$1.5^{+2.0}_{-1.0} \pm 0.2 \pm 0.5$	6.5	0.7σ
4.843	527.29	$4.67^{+2.58}_{-1.92}$	26.7	$7.8^{+4.3}_{-3.2} \pm 0.7 \pm 2.5$	21.1	2.6σ
4.918	208.11	$1.00^{+1.36}_{-0.70}$	22.6	$5.0^{+6.8}_{-3.5} \pm 0.4 \pm 1.6$	21.7	0.7σ
4.951	160.37	$0.00^{+0.95}_{-0.00}$	20.4	$0.0^{+6.8}_{-0.0} \pm 0.0 \pm 0.0$	14.7	-

TABLE II. Relative systematic uncertainties (in %) in the Born cross section measurements at various energy points. The uncertainties caused by the integrated luminosity ($\sigma_{\mathcal{L}}$), the detection efficiency (σ_{ϵ}), the ISR correction factor (σ_{ISR}), the method of signal extraction (σ_{sig}), and their sum in quadrature (σ_{sum}) are listed.

\sqrt{s} (GeV)	$\sigma_{\mathcal{L}}$	σ_{ϵ}	σ_{ISR}	σ_{sig}	σ_{sum}
4.661	1.0	8.1	5.0	1.6	9.7
4.682	1.0	8.1	2.3	1.6	8.6
4.699	1.0	8.1	12.0	1.6	14.6
4.740	1.0	8.1	4.3	1.6	9.4
4.750	1.0	8.2	5.4	1.6	10.0
4.781	1.0	8.3	12.2	1.6	14.9
4.843	1.0	8.3	1.4	1.6	8.6
4.918	1.0	8.4	1.2	1.6	8.7
4.951	1.0	8.5	0.5	1.6	8.7

nisms of the $X(3872)$ provide crucial information about its properties. The observation of a new production process $e^+e^- \rightarrow \omega X(3872)$, combined with the observation of the $X(3872)$ in other production mechanisms, offers an additional window into the composition of the $X(3872)$.

The BESIII collaboration thanks the staff of BEPCII and the IHEP computing center for their strong support. This work is supported in part by National Key R&D Program of China under Contracts Nos. 2020YFA0406300, 2020YFA0406400; National Natural Science Foundation of China (NSFC) under Contracts Nos. 11805090, 12147214, 11635010, 11735014, 11835012, 11935015, 11935016, 11935018, 11961141012, 12022510, 12025502, 12035009, 12035013, 12192260, 12192261, 12192262, 12192263, 12192264, 12192265; Outstanding Research Cultivation Program of Liaoning Normal University No. 21GDL004; the Chinese Academy

of Sciences (CAS) Large-Scale Scientific Facility Program; Joint Large-Scale Scientific Facility Funds of the NSFC and CAS under Contract No. U1832207; the CAS Center for Excellence in Particle Physics (CCEPP); 100 Talents Program of CAS; The Institute of Nuclear and Particle Physics (INPAC) and Shanghai Key Laboratory for Particle Physics and Cosmology; ERC under Contract No. 758462; European Union's Horizon 2020 research and innovation programme under Marie Skłodowska-Curie grant agreement under Contract No. 894790; German Research Foundation DFG under Contracts Nos. 443159800, Collaborative Research Center CRC 1044, GRK 2149; Istituto Nazionale di Fisica Nucleare, Italy; Ministry of Development of Turkey under Contract No. DPT2006K-120470; National Science and Technology fund; National Science Research and Innovation Fund (NSRF) via the Program Management Unit for Human Resources & Institutional Development, Research and Innovation under Contract No. B16F640076; Olle Engkvist Foundation under Contract No. 200-0605; STFC (United Kingdom); Suranaree University of Technology (SUT), Thailand Science Research and Innovation (TSRI), and National Science Research and Innovation Fund (NSRF) under Contract No. 160355; The Royal Society, UK under Contracts Nos. DH140054, DH160214; The Swedish Research Council; U. S. Department of Energy under Contract No. DE-FG02-05ER41374.

-
- [1] S. K. Choi *et al.* (Belle Collaboration), Phys. Rev. Lett. **91**, 262001 (2003).
 - [2] B. Aubert *et al.* (BaBar Collaboration), Phys. Rev. D **71**, 071103 (2005).
 - [3] D. Acosta *et al.* (CDF Collaboration), Phys. Rev. Lett. **93**, 072001 (2004).
 - [4] V. M. Abazov *et al.* (D0 Collaboration), Phys. Rev. Lett. **93**, 162002 (2004).

- [5] R. L. Workman *et al.* (Particle Data Group), PTEP, 2022, 083C01 (2022).
- [6] R. Aaij *et al.* (LHCb Collaboration), Phys. Rev. Lett. **110**, 222001 (2013).
- [7] R. Aaij *et al.* (LHCb Collaboration), JHEP **08**, 123 (2020).
- [8] R. Aaij *et al.* (LHCb Collaboration), Phys. Rev. D **102**, 092005 (2020).
- [9] E. S. Swanson, Phys. Lett. B **598**, 197 (2004); E. S. Swanson, Phys. Rept. **429**, 243 (2006).
- [10] M. Ablikim *et al.* (BESIII Collaboration), Phys. Rev. Lett. **112**, 092001 (2014).
- [11] E. S. Swanson, Phys. Lett. B **598**, 197 (2004); E. S. Swanson, Phys. Rept. **429**, 243 (2006).
- [12] R. Aaij *et al.* (LHCb Collaboration), Eur. Phys. J. C **72**, 1972 (2012).
- [13] S. Chatrchyan *et al.* (CMS Collaboration), JHEP **1304**, 154 (2013).
- [14] M. Aaboud *et al.* (ATLAS Collaboration), JHEP **1701**, 117 (2017).
- [15] M. Ablikim *et al.* (BESIII Collaboration), Phys. Rev. Lett. **114**, 092003 (2015).
- [16] M. Ablikim *et al.* (BESIII Collaboration), Phys. Rev. D **99**, 091103 (2019).
- [17] M. Ablikim *et al.* (BESIII Collaboration), Phys. Rev. D **93**, 011102(R) (2016).
- [18] M. Ablikim *et al.* (BESIII Collaboration), Nucl. Instrum. Meth. A **614**, 345 (2010).
- [19] S. Agostinelli *et al.* (GEANT4 Collaboration), Nucl. Instrum. Meth. A **506**, 250 (2003).
- [20] S. Jadach, B. F. L. Ward and Z. Was, Comp. Phys. Comm. **130**, 260 (2000); Phys. Rev. D **63**, 113009 (2001).
- [21] D. J. Lange, Nucl. Instrum. Meth. A **462**, 152 (2001).
- [22] P. Golonka and Z. Was, Eur. Phys. J. C **45**, 97 (2006).
- [23] X. Zhou, S. Du, G. Li and C. Shen, Comput. Phys. Commun. **258**, 107540 (2021).
- [24] M. Williams, JINST **5**, P09004 (2010).
- [25] E. A. Kuraev and V. S. Fadin, Yad. Fiz. **41**, 733 (1985).
- [26] S. Actis *et al.*, Eur. Phys. J. C **66**, 585 (2010).
- [27] Rolke *et al.*, Nucl. Instrum. Meth. A **551**, 493 (2005).
- [28] M. Ablikim *et al.* (BESIII Collaboration), Phys. Rev. Lett. **118**, 092001 (2017).
- [29] M. Ablikim *et al.* (BESIII Collaboration), Phys. Rev. D **81**, 052005 (2010).
- [30] M. Ablikim *et al.* (BESIII Collaboration), arXiv: 2205.04809.